



Catalytic enantioselective desymmetrizing functionalization of alkyl radicals via Cu(I)/CPA cooperative catalysis

Yong-Feng Cheng^{1,2,5}, Ji-Ren Liu^{3,5}, Qiang-Shuai Gu^{1,2,4,5}, Zhang-Long Yu^{1,2,5}, Jian Wang^{1,2}, Zhong-Liang Li^{2,4}, Jun-Qian Bian^{1,2}, Han-Tao Wen^{1,2}, Xiao-Jing Wang^{1,2}, Xin Hong³✉ and Xin-Yuan Liu^{1,2}✉

In contrast with abundant methods for the asymmetric functionalization of alkyl radicals to generate stereogenic centres at reaction sites, catalytic enantioselective desymmetrizing functionalization of alkyl radicals for forging multiple stereocentres—including positions that are remote from the reaction sites—with both high enantio- and diastereoselectivity remains largely unexplored. The major challenge for such reactions is the high reactivity of open-shell alkyl radicals. Here, we describe a strategy to address this challenge: the use of Cu(II) phosphate to immediately associate with the in situ-generated reactive alkyl radical species, creating a compact and confined chiral microenvironment for effective stereocontrol. With this strategy, we have developed a general and efficient catalytic enantioselective desymmetrizing functionalization of alkene-tethered 1,3-diols. It provides various tetrahydrofurans and analogues bearing multiple stereocentres with remarkably high levels of enantio- and diastereocontrol. Density functional theory calculations and mechanistic experiments revealed a reaction mechanism involving an enantiodetermining outer-sphere C–O bond formation step.

Over the past decade, there has been tremendous progress in the development of catalytic enantioselective radical transformations, providing powerful tools for the sustainable and selective preparation of structurally divergent chiral molecules. Compared with asymmetric catalysis for polar reactions, the unique challenge in this field lies with the enantiocontrol over in situ-generated open-shell alkyl radicals, the high reactivity of which often significantly compromises the influence of chiral catalysts. In this context, innovative catalytic strategies, including the use of Lewis acids^{1,2}, transition metals^{3–9}, organocatalysts^{10,11} and photocatalysts^{12–18}, have spawned powerful synthetic methods to generate stereogenic centres at the immediate reaction centres through close interactions between the catalysts and the open-shell reactive intermediates, together with their reacting partners (Fig. 1a). Despite these exciting advances, the development of catalytic enantioselective desymmetrizing functionalization of alkyl radicals to generate multiple stereocentres both at and away from the reaction sites, with highly selective control of absolute and relative stereochemical configurations, has proven to be a lasting formidable challenge. The major difficulty rests on the lack of competent interactions between reported catalysts and motifs in substrates remote from the reaction sites in the presence of transient alkyl radicals (Fig. 1b). Thus, in contrast with widely explored polar desymmetrization transformations^{19–21}, only a limited number of catalytic enantioselective radical desymmetrization reactions have been disclosed^{22–27}. Moreover, the catalyst-controlled enantiodiscrimination in these reactions has always been done before the functionalization of alkyl radicals, through which the challenging enantiocontrol over alkyl radicals is obviated. In contrast, chiral auxiliary-controlled^{28,29} and

stoichiometric chiral reagent-controlled methods³⁰ have been devised to maintain compact stereodiscriminating transition states with effective communication of stereochemical information. For example, Curran et al.²⁸ have pioneered the use of chiral camphorsultam as the auxiliary for desymmetrizing cyclization of an α -carbonyl alkyl radical to appended cyclohexadiene (Fig. 1c). More recently, Procter and co-workers³⁰ made a great breakthrough using a stoichiometric chiral samarium complex to control the desymmetrizing cyclization of ketyl radicals, affording complex carbocyclic products with excellent stereoselectivity (Fig. 1d). Nonetheless, a catalytic strategy for the abovementioned highly enantioselective desymmetrizing functionalization of alkyl radicals has remained to be developed but is highly desirable for the great potential in expedite generation of structurally diverse chiral molecules with multiple stereocentres (Fig. 1c,d)^{19–21}.

In recent years, since the pioneering studies carried out by Fu and others^{3–5,7,31–33}, chiral transition-metal catalysis using metal species to associate with in situ-generated alkyl radicals through different types of interactions has become a powerful method for radical asymmetric reactions. The interactions between alkyl radicals and transition metals have been believed to be crucial for minimizing uncatalysed background reactions and sustaining high levels of stereocontrol. As a result of our continued interest in Cu(I)-catalysed asymmetric reactions involving radicals^{33–35}, we speculated that such a strategy might be an ideal platform for the development of catalytic enantioselective desymmetrizing functionalization of alkyl radicals. Furthermore, chiral phosphates with well-defined chiral pockets could provide confined microenvironments for the enantiodetermining intermediate to favour the desired transformation

¹Shenzhen Grubbs Institute, Southern University of Science and Technology, Shenzhen, China. ²Department of Chemistry, Southern University of Science and Technology, Shenzhen, China. ³Department of Chemistry, Zhejiang University, Hangzhou, China. ⁴Academy for Advanced Interdisciplinary Studies, Southern University of Science and Technology, Shenzhen, China. ⁵These authors contributed equally: Yong-Feng Cheng, Ji-Ren Liu, Qiang-Shuai Gu, Zhang-Long Yu. ✉e-mail: hxchem@zju.edu.cn; liuxy3@sustech.edu.cn

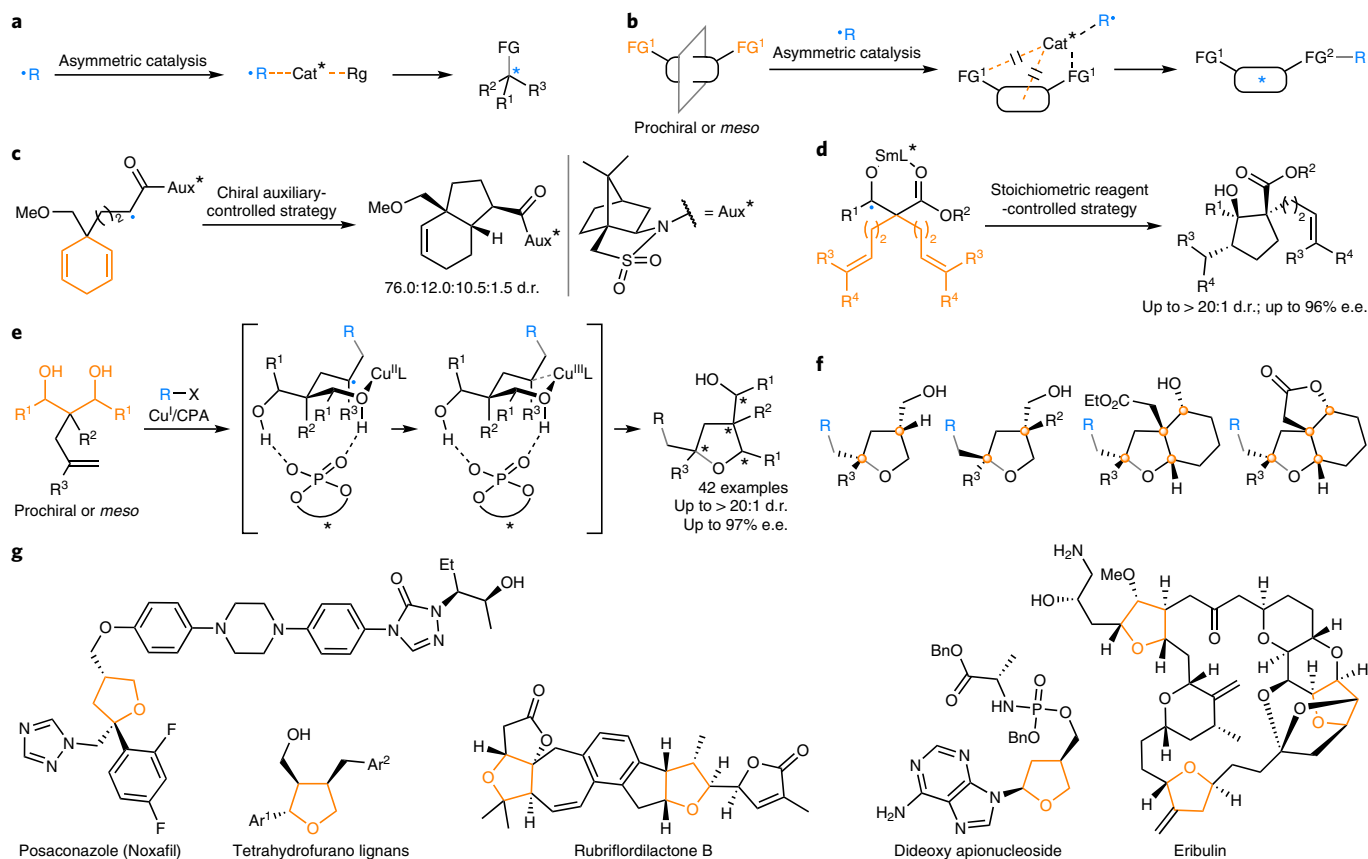


Fig. 1 | Motivation and development of catalytic enantioselective desymmetrizing functionalization of alkyl radicals. **a**, Excellent asymmetric radical catalysis for the generation of chiral centres at the reacting sites relies on close covalent and/or non-covalent interactions (represented as dashed lines) between chiral catalysts (Cat*), alkyl radicals ($\cdot R$) and reagents (Rg). FG, functional group. **b**, The challenges for catalytic enantioselective desymmetrizing functionalization of alkyl radicals lie with competent covalent and/or non-covalent interactions (represented as orange dashed lines) between chiral catalysts and remote motifs away from the reacting functional groups and alkyl radicals, which are commonly compromised by the high reactivity nature of open-shell alkyl radicals. **c,d**, Chiral auxiliary-controlled (**c**) and stoichiometric chiral reagent-controlled strategies (**d**) have been resorted to for realizing enantioselective desymmetrizing functionalization of alkyl radicals, while the corresponding catalytic strategy has remained to be developed. SmL*, samarium complex with (1*R*,1'*R*)-2,2'-(benzylazanediy)bis(1-phenylethan-1-ol). **e**, Our work involves the enantioselective desymmetrizing alkoxylation of alkyl radicals under the cooperative catalysis of Cu(I) and CPA, thus representing a rare catalytic strategy for enantioselective desymmetrizing functionalization of alkyl radicals. **f**, The catalytic methodology provides facile access to sterically congested chiral tetrahydrofurans with up to four tertiary or quaternary stereocentres, three of which are even contiguous, and up to three fused rings. **g**, Chiral tetrahydrofurans are ubiquitous in important natural products (tetrahydrofuran lignans) and medicinally relevant molecules, including posaconazole (Noxafil; an antifungal drug), rubrifordilactone B (an anti-human immunodeficiency virus natural product), dideoxy apionucleoside (an anti-human immunodeficiency virus molecule) and eribulin (Halaven; an anti-cancer drug).

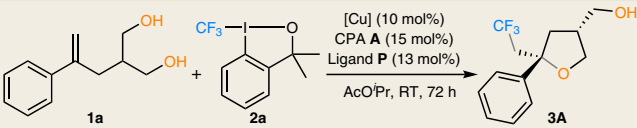
with the simultaneous establishment of multiple stereogenic centres, including positions that are remote to the reaction sites^{36–39}. Accordingly, we envisioned that the use of Cu(I)/chiral phosphoric acid (CPA) cooperative catalysis for asymmetric radical reactions could be translated into a general and practical solution towards the conundrum for catalytic enantioselective desymmetrizing functionalization of alkyl radicals.

Here, we report the discovery of a highly general and efficient catalytic enantioselective desymmetrizing transformation of prochiral or *meso* olefinic 1,3-diols with various radical precursors enabled by Cu(I)/CPA cooperative catalysis (Fig. 1e). The key to success is the robust association of in situ-generated alkyl radical with Cu(II) phosphate in an organized conformation to create a compact chiral microenvironment emanating from the reaction sites, which effectively inhibits strong uncatalysed racemic reactions while exerting effective chirality control over both reaction sites and remote positions. The reaction mechanism and molecular basis of the simultaneous control of multiple stereocentres have been further elucidated with computations, which highlight the synergistic

effects of π - π stacking and hydrogen-bonding interactions in creating the desired compact chiral microenvironment. This discovery provides a highly flexible and practical platform for the rapid assembly of a large array of structurally complex and functionally diverse enantioenriched tetrahydrofurans, as well as their analogues, bearing multiple stereocentres at different positions with remarkably high levels of enantio- and diastereocontrol (Fig. 1f). It is noteworthy that chiral tetrahydrofurans bearing multiple stereogenic centres have been recognized as a functional core unit in both important natural compounds and effective clinical drugs (Fig. 1g), but their diversity-oriented synthesis in a catalytic asymmetric way within one synthetic step remains a significant challenge and scarce^{40–44}.

Results

Reaction design. In our initial efforts, we found that trifluoromethyl-substituted tetrahydrofuran **3A**, bearing two stereocentres, could be obtained in 94% yield from prochiral olefinic 1,3-diol **1a** and Togni's reagent **2a** in the presence of a cooperative catalytic

Table 1 | Optimization of reaction conditions for CPAs and ligands


Reaction scheme showing the conversion of substrate **1a** to product **3a** using CPA **2a** and ligand **P**. Reaction conditions: [Cu] (10 mol%), CPA **A** (15 mol%), Ligand **P** (13 mol%), AcOPr, RT, 72 h.

Chemical structures of CPAs and ligands:

- (*R,R*)-**A1**: R = 4-Ph-C₆H₄
- (*R,R*)-**A2**: R = SiPh₃
- (*R,R*)-**A3**: R = 9-Anth
- (*R,R*)-**A4**: R = Trip
- (*R,R*)-**A5**: R = 4-ⁱBu-C₆H₄
- (*R,R*)-**A6**: R = SiPh₃
- (*R,R*)-**A7**: R = 9-Anth
- (*R,R*)-**A8**: R = Trip
- P1**: 2-CF₃
- P2**: 3-CF₃
- P3**: 4-CF₃
- P4**: R = H
- P5**: R = Et
- P6**: R = Ph
- P7**: R = 4-ⁱBu-C₆H₄

Entry	[Cu]	CPA	Ligand	Yield (%)	d.r.	e.e. (%)
1	CuBH ₄ (PPh ₃) ₂	(<i>R,R</i>)- A1	–	94	1:2	–8/–34
2	CuBH ₄ (PPh ₃) ₂	(<i>R,R</i>)- A2	–	8	1:1	–10/2
3	CuBH ₄ (PPh ₃) ₂	(<i>R,R</i>)- A3	–	86	1:2	0/10
4	CuBH ₄ (PPh ₃) ₂	(<i>R,R</i>)- A4	–	58	1:1	16/5
5	CuBH ₄ (PPh ₃) ₂	(<i>R,R</i>)- A5	–	68	2:1	12/7
6	CuBH ₄ (PPh ₃) ₂	(<i>R,R</i>)- A6	–	4	1:1	5/12
7	CuBH ₄ (PPh ₃) ₂	(<i>R,R</i>)- A7	–	41	2:1	9/10
8	CuBH ₄ (PPh ₃) ₂	(<i>R,R</i>)- A8	–	25	4:1	39/5
9	Cu ₂ O	(<i>R,R</i>)- A8	P1	44	3:1	49/7
10	Cu ₂ O	(<i>R,R</i>)- A8	P2	65	10:1	84/–
11	Cu ₂ O	(<i>R,R</i>)- A8	P3	40	4:1	65/8
12	Cu ₂ O	(<i>R,R</i>)- A8	P4	48	14:1	82/–
13	Cu ₂ O	(<i>R,R</i>)- A8	P5	68	>20:1	86/–
14	Cu ₂ O	(<i>R,R</i>)- A8	P6	78	>20:1	89/–
15 ^a	Cu ₂ O	(<i>R,R</i>)- A8	P7	80	>20:1	91/–
16 ^a	CuBr	(<i>R,R</i>)- A8	P7	85	>20:1	89/–
17	Cu ₂ O	(<i>R,R</i>)- A8	P7^b	86	>20:1	91/–

Reaction conditions: **1a** (0.05 mmol), **2a** (0.075 mmol), [Cu] (10 mol%) and CPA (15 mol%) in AcOPr (0.50 ml) at room temperature (RT) for 72 h. Yield and d.r. values are based on ¹H NMR analysis of the crude products using CH₂Br₂ as an internal standard. Values of e.e. are based on high-performance liquid chromatography analysis. 9-Anth, 9-anthracenyl; Trip, 2,4,6-triisopropylphenyl. ^a7 d. ^b40 mol%.

system of CuBH₄(PPh₃)₂ and 1,1'-bi-2-naphthol (BINOL)-derived CPA (*R,R*)-**A1** (Table 1, entry 1). However, both the diastereoselectivity (2:1) and enantioselectivity (–34/–8% e.e.) were poor. Next, we evaluated a series of BINOL- and 1,1'-spirobiindane-7,7'-diol (SPINOL)-based CPAs with different substituents at the 3,3' positions of the backbones. Unfortunately, these catalysts provided only marginal stereocontrol in this reaction and the use of (*R,R*)-**A8** with 2,4,6-triisopropylphenyl groups at the 3,3' positions proved to be the best in terms of enantioselectivity (Table 1, entries 1–8). However, further extensive efforts to improve the selectivity by screening different Cu salts and organic solvents met with no significant improvement in either diastereo- or enantioselectivity (Supplementary Table 1). Given this, we surmised that an ancillary achiral Lewis base might potentially assist in stereocontrol during the process by influencing the stability of the involved high-valent organo-Cu(II/III) species^{45–48}. Thus, evaluation of various achiral pyridine derivatives (Table 1, entries 9–15) indicated that electron-

deficient pyridines—particularly the 3-substituted ones (entries 10 and 12–15)—were superior ligands for promoting stereoselectivity. Among all of the ligands screened, good results (>20:1 d.r. and 91% e.e.) were obtained with sterically bulky *N,N*-bis(4-(*tert*-butyl)phenyl)nicotinamide **P7** (entry 15), and changing the copper salt to CuBr resulted in a higher yield but slightly lower enantioselectivity (entry 16). Further optimization studies (Supplementary Table 1) revealed that the use of 40 mol% **P7** together with Cu₂O and (*R,R*)-**A8** provided the best results to give **3A** in 86% yield with excellent stereoselectivity (>20:1 d.r.; 91% e.e.) at room temperature for 72 h (entry 17).

With the optimal reaction conditions in hand, we explored the substrate scope of this transformation (Table 2). An array of prochiral olefinic 1,3-diols, including those having mono-substituted phenyl rings with electron-donating or -withdrawing groups at different positions (*ortho*, *meta* or *para*) and a dimethyl-substituted phenyl ring and different bicyclic naphthalene rings on the alkene moiety, could be efficiently transformed into the corresponding trifluoromethyl-substituted tetrahydrofurans **3A–3U** bearing two stereocentres in good yields with high diastereo- and enantioselectivity. Different kinds of common functional groups, such as methoxyl (**3E**), fluoro (**3G** and **3H**), iodo (**3I**), trifluoromethyl (**3J**), ester (**3N**), amide (**3O**), nitrile (**3P**) and nitro (**3Q**), were all compatible with these conditions. It is noteworthy that free aldehyde (**3R**) and primary alcohol (**3S**) are potentially reactive but were also tolerated in this oxidative process. In addition, additional internal double or triple bonds in substrates remained intact in the reaction to deliver products **3T** and **3U**, respectively. This broad compatibility with various functional groups highlights the high generality and synthetic potential of this transformation. Unfortunately, alkyl alkene substrate **1V** did not provide the desired product **3V** under the standard conditions. The absolute configuration of **3A** has been determined by X-ray crystallographic analysis on its sulfonyl derivative (Supplementary Fig. 1), and those of other products in Table 2 were assigned by analogy.

As described above, we were particularly interested in applying this approach to access two congested quaternary stereocentres, the construction of which has long been recognized as an important challenge to the field of chemical synthesis⁴⁹. However, the initial treatment of **4a** under the aforementioned conditions only led to poor enantioselectivity (32% e.e.). This prompted us to examine the bench-stable and inexpensive trifluoromethanesulfonyl chloride (CF₃SO₂Cl) **2b** as an alternative CF₃ source. In this case, Ag₂CO₃ was chosen to quench the in situ-generated HCl by-product, which would otherwise lead to racemic background reactions. After systematic optimization efforts on the evaluation of Cu salts and CPAs (Supplementary Table 2), we identified the bisphosphoric acid (*R,R*)-**A9** developed by Gong and co-workers⁵⁰ as the optimal CPA with no need for any ancillary pyridine ligands. Thus, olefinic 1,3-diols **4a** and **4b** bearing a quaternary stereocentre delivered the corresponding products **5Ab** and **5Bb** in 96 and 91% yields with good stereoselectivity (10:1 and 6:1 d.r.; 83 and 88% e.e.), respectively (Fig. 2). Given the increasing importance of various perfluoroalkyl-containing molecules in the development of pharmaceuticals and agrochemicals as well as materials⁵¹, we thus switched our synthetic targets to the use of perfluorobutanyl sulfonyl chloride **2c** as a radical precursor. Gratifyingly, a diverse range of olefinic 1,3-diols having electronically and functionally diverse phenyl rings on the alkene moiety were all suitable for the reaction in the presence of CuBr (10 mol%) and CPA (*R,R*)-**A9** (15 mol%) (for condition optimization, see Supplementary Table 3), and the desired perfluorobutanyl-substituted tetrahydrofurans **5Ac**, **5Bc** and **5C–5H** bearing two congested quaternary stereocentres were obtained in good yields with high diastereo- and enantioselectivity (Fig. 2). Furthermore, a substrate containing a heterocyclic furan on the alkene moiety readily participated in the reaction to give the product **5I** with excellent

Table 2 | Substrate scope of prochiral olefinic 1,3-diols

 3A , 79% >20:1 d.r., 91% e.e.	 X-ray crystal structure of a derivative of 3A	 3B , 66% >20:1 d.r., 89% e.e. ^a	 3C , 73% >20:1 d.r., 91% e.e.	 3D , 80% >20:1 d.r., 86% e.e.	 3E , 83% >20:1 d.r., 89% e.e. ^a
 3F , 80% >20:1 d.r., 88% e.e.	 3G , 72% >20:1 d.r., 90% e.e. ^a	 3H , 76% >20:1 d.r., 90% e.e. ^a	 3I , 72% >20:1 d.r., 89% e.e.	 3J , 65% >20:1 d.r., 92% e.e.	 3K , 80% >20:1 d.r., 89% e.e. ^a
 3L , 74% >20:1 d.r., 90% e.e. ^a	 3M , 65% 13:1 d.r., 91% e.e. ^a	 3N , 70% >20:1 d.r., 90% e.e.	 3O , 75% >20:1 d.r., 84% e.e. ^a	 3P , 84% >20:1 d.r., 91% e.e. ^a	
 3Q , 82% >20:1 d.r., 92% e.e.	 3R , 71% >20:1 d.r., 87% e.e. ^a	 3S , 79% 14:1 d.r., 88% e.e.	 3T , 70% >20:1 d.r., 86% e.e.	 3U , 78% >20:1 d.r., 90% e.e.	 3V , 0%

Reaction conditions: **1a** (0.2 mmol), **2a** (0.3 mmol), Cu₂O (10 mol%), (*R*)-**A8** (15 mol%) and **P7** (40 mol%) in AcOPr (1.0 ml) at room temperature for 72 h. Isolated yields are shown. Values of d.r. and e.e. were determined by ¹H NMR and high-performance liquid chromatography analysis, respectively. ^a50 °C. Ad, 1-adamantyl.

result. In addition, no detrimental effects to the efficiency and stereoselectivity of this process were observed with substrates bearing different mono-substituted phenyl rings, a polyarene naphthalene ring and aromatic heterocycles (**5J**–**5P**) in the tether. The tolerance of heterocycles, which are privileged motifs in medicines, is significant in that it allows for potential application in drug discovery.

To demonstrate the synthetic utility of this methodology, the resultant compound **5J**, bearing a bromide-containing aromatic ring, was converted to valuable spiro-heterocycle **6** bearing two chiral tetrasubstituted carbons in 65% yield (Fig. 2), which has great potential for further transformation into other important bioactive compounds⁵². Meanwhile, it is striking to note that the iodine(III) reagent azidoiodinane (**2d**) could also be employed as a radical precursor. Thus, the desired azido-substituted tetrahydrofuran **7** bearing two congested quaternary stereocentres was delivered in the presence of CuBH₄(PPh₃)₂ (10 mol%) and (*R*)-**A10** (15 mol%) in CCl₄ at room temperature in good yield with promising stereoselectivity control (Fig. 2). The reaction is currently under further optimization in our laboratory. The obtained skeleton resembles the core of the broad-spectrum, orally active azole antifungal drug posaconazole (Noxafil) (Fig. 1g). The relative and absolute configurations of **6** have been determined by a combination of two-dimensional NMR analysis and chiroptical methods (see Supplementary Information for details) and further confirmed by X-ray crystallographic analysis. The configurations of products **5** and **7** in Fig. 2 were assigned by analogy thereafter.

Reaction development for *meso* substrates. We then sought to examine the possibility of using *meso* olefinic 1,3-diols for the rapid synthesis of more complex chiral heterocyclic rings with four stereocentres, including two chiral tetrasubstituted carbons. Thus, systematic optimization of different reaction parameters, including catalysts, additional ligands, solvents and temperature (Supplementary Table 4), was carried out. To our delight, a simple desymmetrization procedure for the highly efficient formation of chiral bicyclic rings **9A** and **9B** was successfully realized from *meso* 1,3-diols in the presence of CuTc (10 mol%), CPA (*R,R*)-**A9** (15 mol%) and PPh₃ (20 mol%) as an ancillary ligand with good results (Table 3). Furthermore, treatment of the obtained products **9A** and **9B** with *p*-toluenesulfonic acid (1.0 equiv.) provided valuable 5-5-6 fused rings **10A** and **10B** with good yields through an intramolecular transesterification reaction. Thus, this process provides an attractive approach with which to quickly and efficiently construct building blocks with multiple contiguous stereocentres, which is especially attractive in complex natural product synthesis. The relative and absolute configurations of **10A** have been determined by a combination of two-dimensional NMR analysis and chiroptical methods (see Supplementary Information for details), and other products in Table 3 were assigned by analogy thereafter.

Mechanistic investigations. A series of control experiments were conducted to gain insights into the reaction mechanism. First, the present reaction was completely inhibited by the addition of

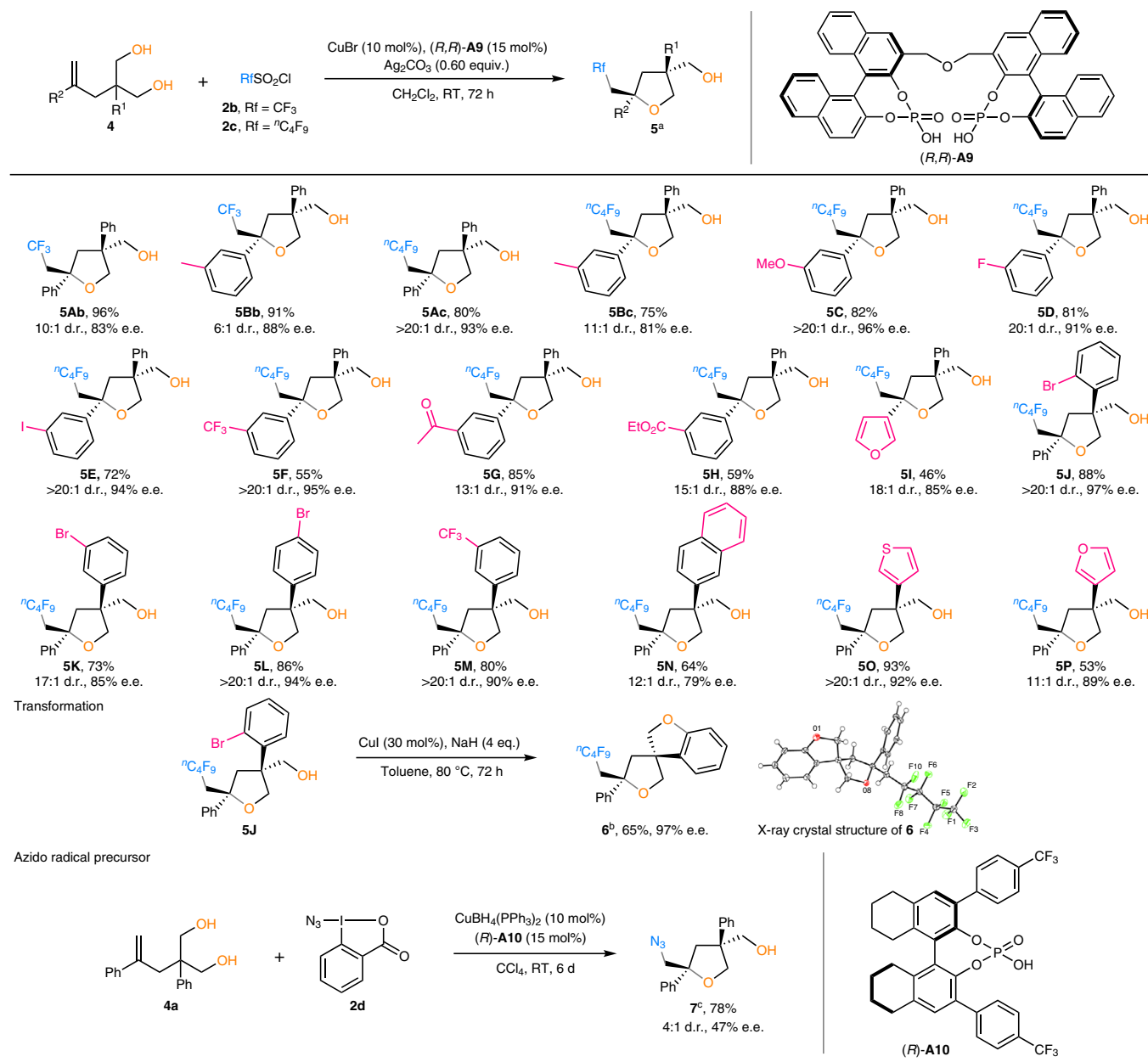
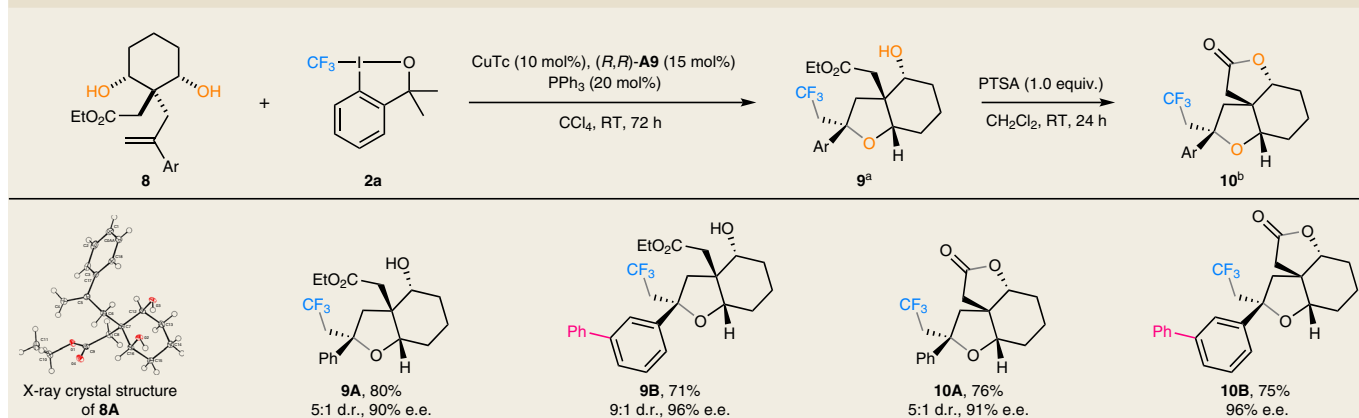


Fig. 2 | Substrate scope to access two congested quaternary stereocentres with different radicals. ^aReaction conditions: **4** (0.1 mmol), **2b** or **2c** (0.12 mmol), CuBr (10 mol%), (R,R)-**A9** (15 mol%), and Ag₂CO₃ (0.6 equiv.) in CH₂Cl₂ (1.0 ml) at room temperature for 72 h under argon. Isolated yields were shown. Values of d.r. and e.e. were determined by ¹H NMR and high-performance liquid chromatography analysis, respectively. ^bReaction conditions: **5J** (0.08 mmol), CuI (30 mol%), and NaH (4.0 equiv.) in toluene (1.0 ml) at 80 °C for 72 h. ^cReaction conditions: **4a** (0.1 mmol), **2d** (0.12 mmol), CuBH₄(PPh₃)₂ (10 mol%) and (R)-**A10** (15 mol%) in CCl₄ (1.0 ml) at room temperature for 6 d under argon.

2,2,6,6-tetramethyl-1-piperidinyloxy (TEMPO) and largely by 2,6-di-*tert*-butyl-4-methylphenol (BHT). In addition, the radical trapping product CF₃-TEMPO **11** was observed in the former experiment (Fig. 3a). These observations, together with previous mechanistic studies^{35,53}, suggest that a free radical •CF₃ is probably generated in situ via single-electron transfer (SET) between Cu(I) and radical precursors. Subsequent free radical addition to an alkene⁷ and complexation with Cu(II)/chiral phosphate³⁵ gives rise to alkyl radical intermediate **I** (Fig. 3c). In addition, we observed a linear relationship between the enantiopurities of the products and corresponding catalysts, respectively, indicating the involvement of one CPA catalyst in each enantiodetermining transition state (Fig. 3b). Therefore, in principle, there exist three possible C–O bond

formation pathways from the in situ-generated Cu(II)-coordinated alkyl radical intermediate **I**, as depicted in Fig. 3c. Path A is the radical substitution via direct attack of the Cu-bonded alkoxy group by the alkyl radical, which is essentially an S_H2 reaction at oxygen⁵⁴. The other two pathways involve either a carbocation intermediate via a SET process (path B) or an alkylcopper(III) intermediate from radical capture, followed by reductive elimination (path C). To further elaborate the mechanistic details of this radical desymmetrizing functionalization reaction and to account for the origins of the observed excellent diastereo- and enantioselectivity, density functional theory (DFT) calculations were then performed.

The DFT-computed free energy profile of the C–O bond formation process is shown in Fig. 4. From the benzyl radical intermediate

Table 3 | Substrate scope of *meso* olefinic 1,3-diols and transformation

^aReaction conditions: **8** (0.1 mmol), **2a** (0.15 mmol), CuTc (10 mol%), (*R,R*)-**A9** (15 mol%) and PPh₃ (20 mol%) in CCl₄ (1.0 ml) at room temperature for 72 h. Isolated yields are shown. Values of d.r. and e.e. were determined by ¹H NMR and high-performance liquid chromatography analysis, respectively. ^bReaction conditions: **9** (1.0 equiv.) and *p*-toluenesulfonic acid (PTSA; 1.0 equiv.) in CH₂Cl₂ (0.05 M) at room temperature for 24 h.

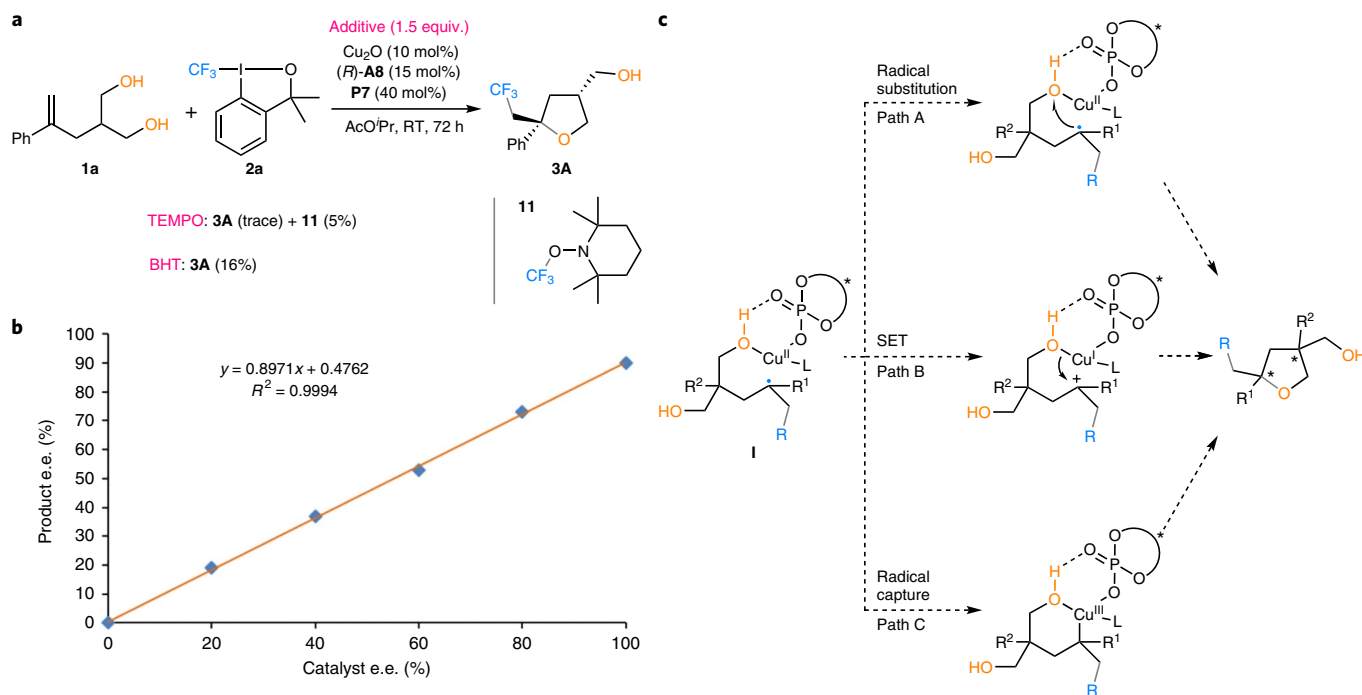


Fig. 3 | Mechanistic studies of the catalytic enantioselective desymmetrizing functionalization reactions involving radical species. a, Radical trapping experiments. **b**, Nonlinear effect study results. **c**, Possible pathways for the enantiodetermining C–O bond formation.

Int12, the radical bonds to the Cu(II)-CPA species **Int13** to generate the Cu(III) intermediate **Int14**, which is the proposed Cu(III) species in path C of Fig. 3c. We want to emphasize that the CPA anion is not directly coordinated to copper in **Int14**, due to the multiple hydrogen-bonding interactions with diol. From **Int14**, although a classic concerted C–O reductive elimination seems likely, we cannot locate such transition states despite extensive efforts. Instead, a very facile stepwise reductive elimination pathway was identified. The Cu(III) intermediate **Int14** undergoes a barrierless heterolytic cleavage of the C–Cu bond via **TS15**, leading to the Cu(I) intermediate **Int16** with a benzyl cation. This intermediate **Int16** is involved in the proposed SET process (Fig. 3c, path B). Subsequent C–O bond formation via **TS17** produces the desymmetrization product **3A** and regenerates

the Cu(I) catalyst. Therefore, the overall C–O bond formation is a stepwise process involving both the proposed Cu(III) species (Fig. 3c, path C) and Cu(I) species (Fig. 3c, path B). The copper-containing intermediates and transition states in Fig. 4 are all closed-shell singlet species except for Cu(II) species **Int13**. The triplet state of **Int16** is significantly less favourable, which excludes the proposed path A involving radical substitution (Supplementary Fig. 4).

The mechanistic model provides a molecular basis with which to understand the controlling factors of stereoselectivity^{55,56}. Optimized structures and energies of the competing C–O bond formation transition states are shown in Fig. 5. Extensive conformational searches were performed on the C–O bond formation transition states to ensure that the most stable conformers were located, and

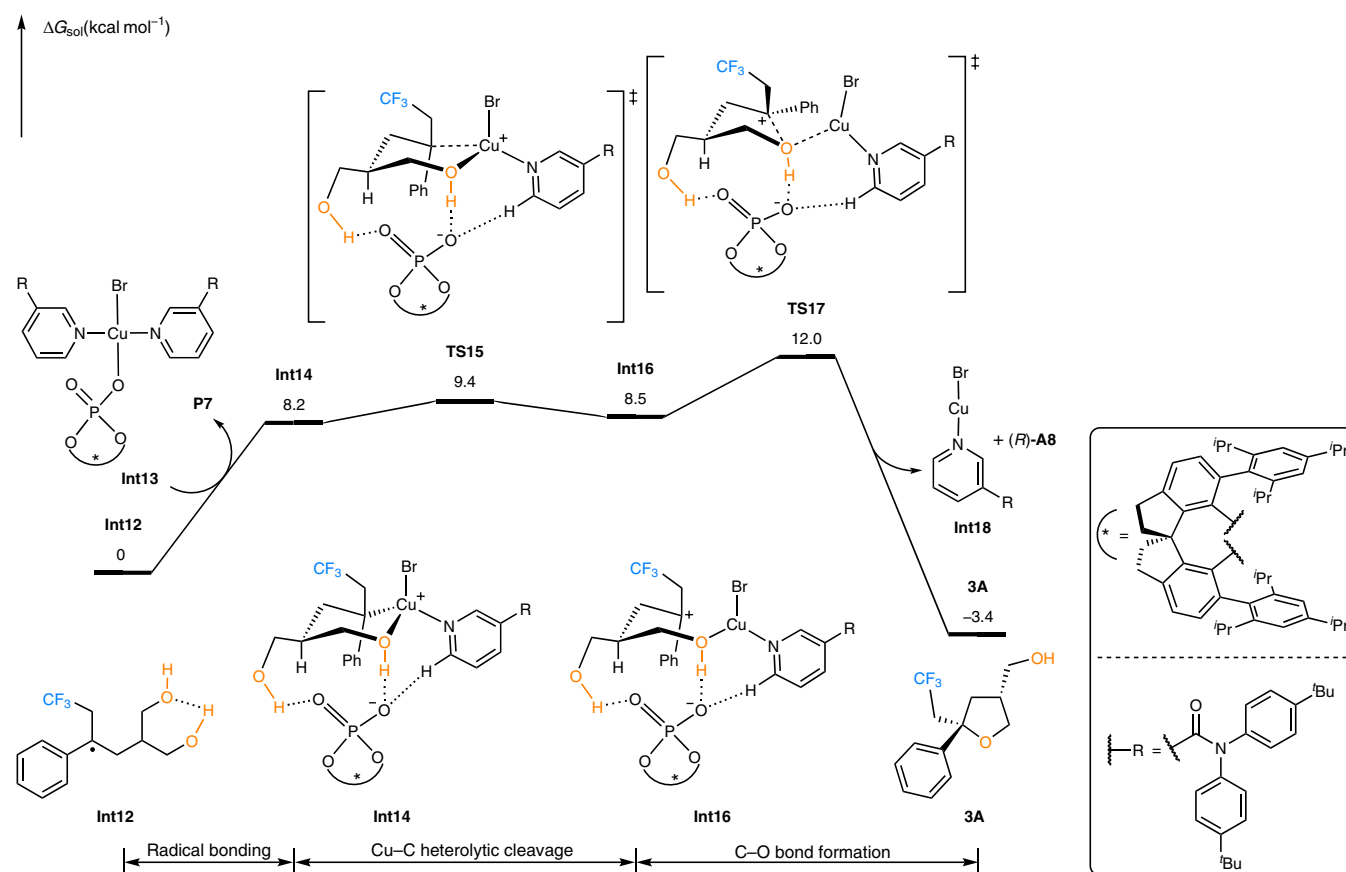


Fig. 4 | DFT-computed free energy profile of the favoured C–O bond formation process. Computational studies were performed at the B3LYP-D3(BJ)/6-311+G(d,p)-SDD-SMD(Propyl Ethanoate)//B3LYP-D3(BJ)/6-31G(d)-LANL2DZ level of theory. This process involves sequential radical bonding, Cu–C bond heterolytic cleavage and C–O bond formation.

unfavourable conformers are included in Supplementary Figs. 5–8. **TS17** is at least 3.5 kcal mol^{−1} more favourable than the other three transition states (**TS17-a**, **TS17-b** and **TS17-c**), which is consistent with the excellent enantio- and diastereoselectivities in the experiments. Comparing **TS17** and **TS17-a**, the π – π stacking interaction between the coordinating Lewis base and the phenyl group of the substrate determines the stereoselectivity of the benzylic position⁵⁷. This π – π stacking interaction is confirmed based on the calculations of interacting fragments, as well as independent gradient model (IGM) analysis⁵⁸ (see Supplementary Fig. 9). The same stabilizing π – π stacking is not able to exist in **TS17-a** because the phenyl group is distal to pyridine. Thus, the Lewis base acts as a bridge to transfer the chirality of the CPA anion to the remote benzylic stereocentre. This highlights the key role of the Lewis base in the control of stereoselectivity, as was found in the experiments (see Table 1). The second stereoselectivity-controlling factor is the hydrogen-bonding network between the diol and CPA anion. In the favoured transition state **TS17**, the two hydroxymethyl groups are *anti*, as in the highlighted Newman projection. The same two groups are *gauche* in **TS17-b** and **TS17-c** due to the change of the tertiary stereogenic centre, which disfavours these two transition states. Our calculations highlight the synergistic effects of π – π stacking and the hydrogen-bonding network, which create the desired chiral microenvironment, leading to the remarkable differentiation of four competing transition states and excellent control of multiple stereocentres.

Conclusions

In summary, we have developed a highly general and efficient strategy to enable a rare catalytic enantioselective desymmetrizing

functionalization of alkyl radicals by the use of Cu(I)/CPA cooperative catalysis. The key to success is the use of Cu(II) phosphate to immediately associate with alkyl radical species in an organized conformation to create a compact and well-defined chiral microenvironment. Thus, strong uncatalysed racemic reactions are readily inhibited and effective stereocontrol is exerted to realize catalytic enantioselective desymmetrizing functionalization of prochiral or *meso* olefinic 1,3-diols with various radical precursors. This discovery provides a highly flexible and practical platform for the rapid assembly of a large array of structurally complex and functionally diverse enantioenriched tetrahydrofurans, as well as their analogues, bearing multiple stereocentres with up to four congested stereocentres and remarkably high levels of enantio- and diastereocontrol. Computational studies reveal an outer-sphere C–O bond formation as the enantioselectivity-determining step. The hydrogen-bonding network with the CPA anion, and the π – π stacking interaction with the pyridine Lewis base, synergistically create a compact chiral environment, which is able to differentiate multiple stereocentres to achieve excellent stereocontrol. We anticipate that the present approach will find broad applications in synthetic and medicinal chemistry, and the mechanistic insights may promote further developments in related challenging catalytic radical desymmetrization transformations in the future.

Methods

Synthesis of 3 by Cu(I)/CPA/Lewis base. Under argon, an oven-dried re-sealable Schlenk tube equipped with a magnetic stir bar was charged with substrate **1** (0.2 mmol; 1.0 equiv.), Cu₂O (2.9 mg; 0.02 mmol; 10 mol%), CPA (*R*)-**A8** (21.6 mg; 0.03 mmol; 15 mol%), **P7** (30.9 mg; 0.08 mmol; 40 mol%), Togni's reagent **2a**

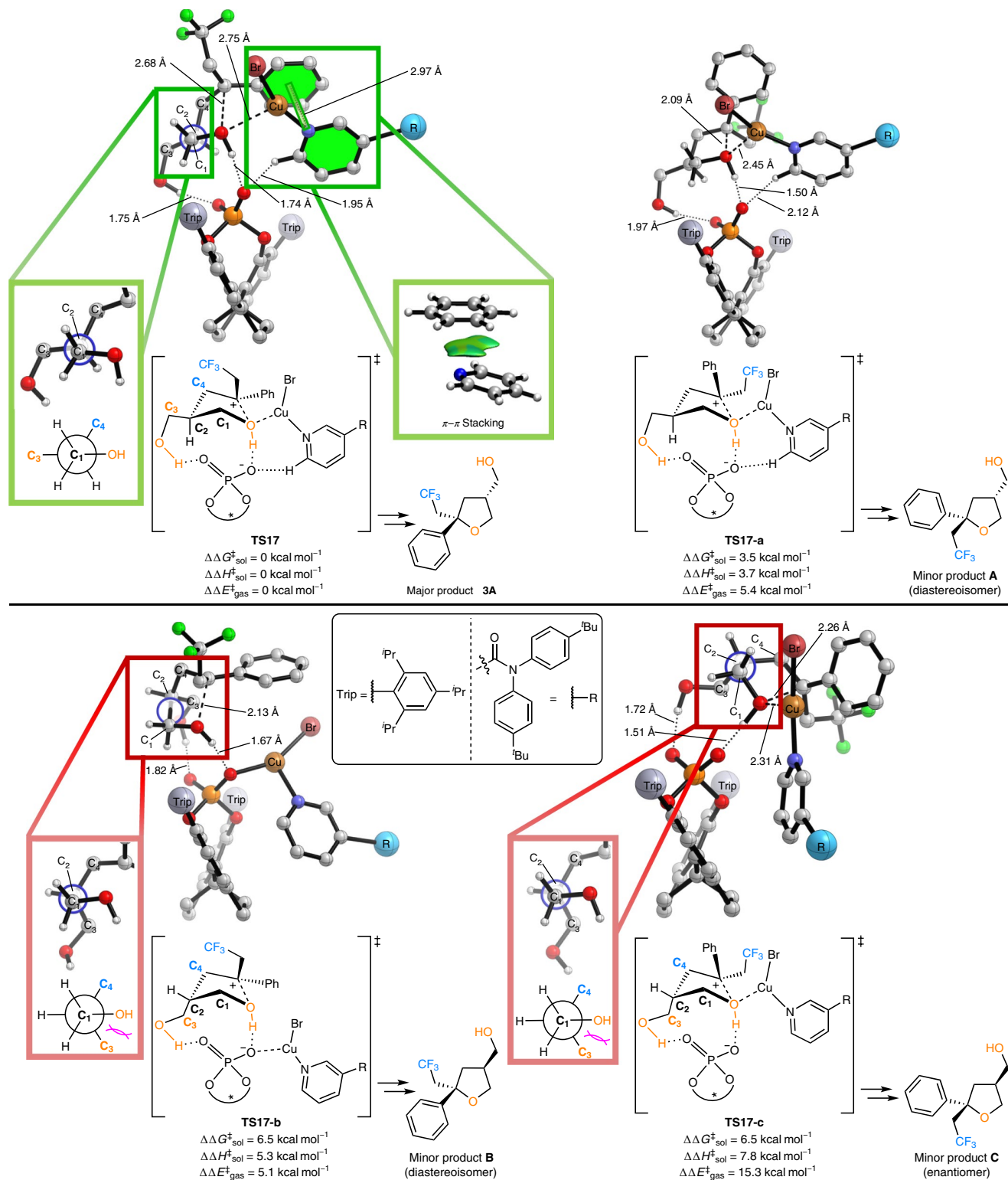


Fig. 5 | DFT-computed enantioselectivity-determining C–O bond formation transition states. Computational studies were performed at the B3LYP-D3(BJ)/6-311+G(d,p)-SDD-SMD(Propyl Ethanoate)//B3LYP-D3(BJ)/6-31G(d)-LANL2DZ level of theory. Trivial hydrogens have been omitted from the three-dimensional diagram for clarity. Transition state **TS17** is energetically most favourable, which is in agreement with the experimental results. Non-covalent interactions, such as π – π stacking between the coordinating Lewis base and the alkenyl phenyl ring in the substrate, and hydrogen-bonding between diol and the CPA anion, synergistically provide the desired compact and confined microenvironment for effective enantiodiscrimination.

(99.0 mg; 0.3 mmol; 1.5 equiv.) and AcO^iPr (2.0 ml) at 25°C. The sealed tube was then stirred at 25°C. Upon completion (monitored by thin-layer chromatography (TLC)), the solvent was removed in vacuo and the residue was purified by silica gel chromatography to afford the desired product **3**.

Synthesis of **5 by Cu(I)/CPA.** Under argon, an oven-dried re-sealable Schlenk tube equipped with a magnetic stir bar was charged with substrate **4** (0.1 mmol; 1.0 equiv.), CuBr (1.4 mg; 0.01 mmol; 10 mol%), CPA (*R,R*)-**A9** (11.1 mg; 0.015 mmol; 15 mol%), **2b** (20.2 mg; 0.12 mmol; 1.2 equiv.) or **2c** (38.2 mg;

0.12 mmol; 1.2 equiv.), Ag_2CO_3 (16.5 mg; 0.06 mmol; 0.6 equiv.) and CH_2Cl_2 (1.0 mL) at 25 °C. The sealed tube was then stirred at 25 °C. Upon completion (monitored by TLC), the solvent was removed in vacuo and the residue was purified by silica gel chromatography to afford the desired product **5**.

Synthesis of 9 by Cu(I)/CPA/PPH₃. Under argon, an oven-dried re-sealable Schlenk tube equipped with a magnetic stir bar was charged with substrate **8** (0.1 mmol; 1.0 equiv.), CuTc (0.01 mmol; 1.9 mg; 10 mol%), (*R,R*)-**A9** (11.1 mg; 0.015 mmol; 15 mol%), PPH_3 (5.2 mg; 0.02 mmol; 20 mol%) Togni's reagent **2a** (49.5 mg; 0.15 mmol; 1.5 equiv.) and CCl_4 (1.0 mL) at 25 °C. The sealed tube was then stirred at 25 °C. Upon completion (monitored by TLC), the solvent was removed in vacuo and the residue was purified by silica gel chromatography to afford the desired product **9**.

Data availability

Data relating to the materials and methods, optimization studies, experimental procedures, mechanistic studies and DFT calculations, high-performance liquid chromatography spectra, NMR spectra and mass spectrometry are available in the Supplementary Information. Crystallographic data for compounds **3A'**, **6** and **8A** are available free of charge from the Cambridge Crystallographic Data Centre under reference numbers 1916711 (**3A'**), 1922870 (**6**) and 1916714 (**8A**). All other data are available from the authors upon reasonable request.

Received: 30 May 2019; Accepted: 7 February 2020;

Published online: 16 March 2020

References

- Sibi, M. P. & Porter, N. A. Enantioselective free radical reactions. *Acc. Chem. Res.* **32**, 163–171 (1999).
- Brimioule, R. & Bach, T. Enantioselective Lewis acid catalysis of intramolecular enone [2+2] photocycloaddition reactions. *Science* **342**, 840–843 (2013).
- Choi, J. & Fu, G. C. Transition metal-catalyzed alkyl–alkyl bond formation: another dimension in cross-coupling chemistry. *Science* **356**, eaaf7230 (2017).
- Fu, G. C. Transition-metal catalysis of nucleophilic substitution reactions: a radical alternative to $\text{S}_{\text{N}}1$ and $\text{S}_{\text{N}}2$ processes. *ACS Cent. Sci.* **3**, 692–700 (2017).
- Cherney, A. H., Kadunce, N. T. & Reisman, S. E. Enantioselective and enantiospecific transition-metal-catalyzed cross-coupling reactions of organometallic reagents to construct C–C bonds. *Chem. Rev.* **115**, 9587–9652 (2015).
- Chemler, S. R., Karyakarte, S. D. & Khoder, Z. M. Stereoselective and regioselective synthesis of heterocycles via copper-catalyzed additions of amine derivatives and alcohols to alkenes. *J. Org. Chem.* **82**, 11311–11325 (2017).
- Zhu, R. & Buchwald, S. L. Enantioselective functionalization of radical intermediates in redox catalysis: copper-catalyzed asymmetric oxytrifluoromethylation of alkenes. *Angew. Chem. Int. Ed.* **52**, 12655–12658 (2013).
- Jiang, H., Lang, K., Lu, H., Wojtas, L. & Zhang, X. P. Asymmetric radical bicyclization of allyl azidoformates via cobalt(II)-based metalloradical catalysis. *J. Am. Chem. Soc.* **139**, 9164–9167 (2017).
- Hao, W., Harenberg, J. H., Wu, X., MacMillan, S. N. & Lin, S. Diastereo- and enantioselective formal [3+2] cycloaddition of cyclopropyl ketones and alkenes via Ti-catalyzed radical redox relay. *J. Am. Chem. Soc.* **140**, 3514–3517 (2018).
- Beeson, T. D., Mastracchio, A., Hong, J.-B., Ashton, K. & MacMillan, D. W. C. Enantioselective organocatalysis using SOMO activation. *Science* **316**, 582–585 (2007).
- Hashimoto, T., Kawamata, Y. & Maruoka, K. An organic thiyl radical catalyst for enantioselective cyclization. *Nat. Chem.* **6**, 702–705 (2014).
- Nicewicz, D. A. & MacMillan, D. W. C. Merging photoredox catalysis with organocatalysis: the direct asymmetric alkylation of aldehydes. *Science* **322**, 77–80 (2008).
- Arceo, E., Jurberg, I. D., Álvarez-Fernández, A. & Melchiorre, P. Photochemical activity of a key donor–acceptor complex can drive stereoselective catalytic α -alkylation of aldehydes. *Nat. Chem.* **5**, 750–756 (2013).
- Rono, L. J., Yayla, H. G., Wang, D. Y., Armstrong, M. F. & Knowles, R. R. Enantioselective photoredox catalysis enabled by proton-coupled electron transfer: development of an asymmetric aza-pinacol cyclization. *J. Am. Chem. Soc.* **135**, 17735–17738 (2013).
- Huo, H. et al. Asymmetric photoredox transition-metal catalysis activated by visible light. *Nature* **515**, 100–103 (2014).
- Du, J., Skubi, K. L., Schultz, D. M. & Yoon, T. P. A dual-catalysis approach to enantioselective [2+2] photocycloadditions using visible light. *Science* **344**, 392–396 (2014).
- Proctor, R. S. J., Davis, H. J. & Phipps, R. J. Catalytic enantioselective Minisci-type addition to heteroarenes. *Science* **360**, 419–422 (2018).
- Fu, M.-C., Shang, R., Zhao, B., Wang, B. & Fu, Y. Photocatalytic decarboxylative alkylations mediated by triphenylphosphine and sodium iodide. *Science* **363**, 1429–1434 (2019).
- Zeng, X.-P., Cao, Z.-Y., Wang, Y.-H., Zhou, F. & Zhou, J. Catalytic enantioselective desymmetrization reactions to all-carbon quaternary stereocenters. *Chem. Rev.* **116**, 7330–7396 (2016).
- Saint-Denis, T. G., Zhu, R.-Y., Chen, G., Wu, Q.-F. & Yu, J.-Q. Enantioselective $\text{C}(\text{sp}^3)$ -H bond activation by chiral transition metal catalysts. *Science* **359**, eaao4798 (2018).
- Mettrano, A. J. & Miller, S. J. Peptide-based catalysts reach the outer sphere through remote desymmetrization and atroposelectivity. *Acc. Chem. Res.* **52**, 199–215 (2019).
- Ye, K.-Y., McCallum, T. & Lin, S. Bimetallic radical redox-relay catalysis for the isomerization of epoxides to allylic alcohols. *J. Am. Chem. Soc.* **141**, 9548–9554 (2019).
- Zhao, Y. & Weix, D. J. Enantioselective cross-coupling of *meso*-epoxides with aryl halides. *J. Am. Chem. Soc.* **137**, 3237–3240 (2015).
- Gansäuer, A., Fan, C.-A., Keller, F. & Karbaum, P. Regiodivergent epoxide opening: a concept in stereoselective catalysis beyond classical kinetic resolutions and desymmetrizations. *Chem. Eur. J.* **13**, 8084–8090 (2007).
- Stache, E. E., Ravis, T. & Doyle, A. G. Dual nickel- and photoredox-catalyzed enantioselective desymmetrization of cyclic *meso*-anhydrides. *Angew. Chem. Int. Ed.* **56**, 3679–3683 (2017).
- Bovino, M. T. et al. Enantioselective copper-catalyzed carboetherification of unactivated alkenes. *Angew. Chem. Int. Ed.* **53**, 6383–6387 (2014).
- Milan, M., Bietti, M. & Costas, M. Enantioselective aliphatic C–H bond oxidation catalyzed by bioinspired complexes. *Chem. Commun.* **54**, 9559–9570 (2018).
- Curran, D. P., Geib, S. J. & Lin, C.-H. Group selective radical cyclizations with Oppolzer's camphor sultam. *Tetrahedron Asymmetry* **5**, 199–202 (1994).
- Villar, F., Kolly-Kovac, T., Equey, O. & Renaud, P. Highly stereoselective radical cyclization of haloacetals controlled by the acetal center. *Chem. Eur. J.* **9**, 1566–1577 (2003).
- Kern, N., Plesniak, M. P., McDouall, J. J. W. & Procter, D. J. Enantioselective cyclizations and cyclization cascades of samarium ketyl radicals. *Nat. Chem.* **9**, 1198–1204 (2017).
- Zhang, W. et al. Enantioselective cyanation of benzylic C–H bonds via copper-catalyzed radical relay. *Science* **353**, 1014–1018 (2016).
- Wang, Z., Yin, H. & Fu, G. C. Catalytic enantioconvergent coupling of secondary and tertiary electrophiles with olefins. *Nature* **563**, 379–383 (2018).
- Lin, J.-S. et al. A dual-catalytic strategy to direct asymmetric radical aminotrifluoromethylation of alkenes. *J. Am. Chem. Soc.* **138**, 9357–9360 (2016).
- Dong, X.-Y. et al. A general asymmetric copper-catalysed Sonogashira $\text{C}(\text{sp}^3)$ – $\text{C}(\text{sp})$ coupling. *Nat. Chem.* **11**, 1158–1166 (2019).
- Gu, Q.-S., Li, Z.-L. & Liu, X.-Y. Copper(I)-catalyzed asymmetric reactions involving radicals. *Acc. Chem. Res.* **53**, 170–181 (2020).
- Phipps, R. J., Hamilton, G. L. & Toste, F. D. The progression of chiral anions from concepts to applications in asymmetric catalysis. *Nat. Chem.* **4**, 603–614 (2012).
- Parmar, D., Sugiono, E., Raja, S. & Rueping, M. Complete field guide to asymmetric BINOL-phosphate derived Brønsted acid and metal catalysis: history and classification by mode of activation; Brønsted acidity, hydrogen bonding, ion pairing, and metal phosphates. *Chem. Rev.* **114**, 9047–9153 (2014).
- Wang, Z., Chen, Z. & Sun, J. Catalytic asymmetric nucleophilic openings of 3-substituted oxetanes. *Org. Biomol. Chem.* **12**, 6028–6032 (2014).
- Akiyama, T. & Mori, K. Stronger Brønsted acids: recent progress. *Chem. Rev.* **115**, 9277–9306 (2015).
- Kauffman, C. A., Malani, A. N., Easley, C. & Kirkpatrick, P. Posaconazole. *Nat. Rev. Drug Discov.* **6**, 183–184 (2007).
- Umezawa, T. Diversity in lignan biosynthesis. *Phytochem. Rev.* **2**, 371–390 (2003).
- Xiao, W.-L. et al. Rubrifloridilactones A and B, two novel bisnortriterpenoids from *Schisandra rubriflora* and their biological activities. *Org. Lett.* **8**, 991–994 (2006).
- Toti, K. S. et al. Synthesis of an apionucleoside family and discovery of a prodrug with anti-HIV activity. *J. Org. Chem.* **79**, 5097–5112 (2014).
- Lorente, A., Lamariano-Merketegi, J., Albericio, F. & Álvarez, M. Tetrahydrofuran-containing macrolides: a fascinating gift from the deep sea. *Chem. Rev.* **113**, 4567–4610 (2013).
- Hickman, A. J. & Sanford, M. S. High-valent organometallic copper and palladium in catalysis. *Nature* **484**, 177–185 (2012).
- Vogl, E. M., Gröger, H. & Shibasaki, M. Towards perfect asymmetric catalysis: additives and cocatalysts. *Angew. Chem. Int. Ed.* **38**, 1570–1577 (1999).
- Hong, L., Sun, W., Yang, D., Li, G. & Wang, R. Additive effects on asymmetric catalysis. *Chem. Rev.* **116**, 4006–4123 (2016).
- Cheng, Y.-F., Dong, X.-Y., Gu, Q.-S., Yu, Z.-L. & Liu, X.-Y. Achiral pyridine ligand-enabled enantioselective radical oxytrifluoromethylation of alkenes with alcohols. *Angew. Chem. Int. Ed.* **56**, 8883–8886 (2017).
- Quasdorf, K. W. & Overman, L. E. Catalytic enantioselective synthesis of quaternary carbon stereocenters. *Nature* **516**, 181–191 (2014).

50. Chen, X.-H., Zhang, W.-Q. & Gong, L.-Z. Asymmetric organocatalytic three-component 1,3-dipolar cycloaddition: control of stereochemistry via a chiral Brønsted acid activated dipole. *J. Am. Chem. Soc.* **130**, 5652–5653 (2008).
51. Ni, C., Hu, M. & Hu, J. Good partnership between sulfur and fluorine: sulfur-based fluorination and fluoroalkylation reagents for organic synthesis. *Chem. Rev.* **115**, 765–825 (2015).
52. Aho, J. E., Pihko, P. M. & Rissa, T. K. Nonanomeric spiroketals in natural products: structures, sources, and synthetic strategies. *Chem. Rev.* **105**, 4406–4440 (2005).
53. Charpentier, J., Früh, N. & Togni, A. Electrophilic trifluoromethylation by use of hypervalent iodine reagents. *Chem. Rev.* **115**, 650–682 (2015).
54. Gephart, R. T. et al. Reaction of Cu^I with dialkyl peroxides: Cu^{II}-alkoxides, alkoxy radicals, and catalytic C–H etherification. *J. Am. Chem. Soc.* **134**, 17350–17353 (2012).
55. Reid, J. P., Simón, L. & Goodman, J. M. A practical guide for predicting the stereochemistry of bifunctional phosphoric acid catalyzed reactions of imines. *Acc. Chem. Res.* **49**, 1029–1041 (2016).
56. Duarte, F. & Paton, R. S. Molecular recognition in asymmetric counteranion catalysis: understanding chiral phosphate-mediated desymmetrization. *J. Am. Chem. Soc.* **139**, 8886–8896 (2017).
57. Wheeler, S. E. Understanding substituent effects in noncovalent interactions involving aromatic rings. *Acc. Chem. Res.* **46**, 1029–1038 (2013).
58. Lefebvre, C. et al. Accurately extracting the signature of intermolecular interactions present in the NCI plot of the reduced density gradient versus electron density. *Phys. Chem. Chem. Phys.* **19**, 17928–17936 (2017).

Acknowledgements

Financial support from the National Natural Science Foundation of China (21722203 and 21831002 to X.-Y.L., 21702182 and 2187308 to X.H. and 21801116 to Z.-L.L.),

Shenzhen Special Funds (JCYJ20170412152435366 and JCYJ20170307105638498 to X.-Y.L.), Shenzhen Nobel Prize Scientists Laboratory Project (C17783101 to X.-Y.L.) and 'Fundamental Research Funds for the Central Universities' (2019QNA3009, X.H.) are gratefully acknowledged. Calculations were performed on the high-performance computing system at the Department of Chemistry, Zhejiang University.

Author contributions

X.-Y.L. conceived of and supervised the project. Y.-F.C., Z.-L.Y., J.W., Q.-S.G. and Z.-L.L. designed the experiments and analysed the data. Y.-F.C., Z.-L.Y., J.W., J.-Q.B., H.-T.W. and X.-J.W. performed the experiments. J.-R.L. and X.H. designed and performed the DFT calculations. X.-Y.L., X.H. and Q.-S.G. wrote the paper. All authors discussed the results and commented on the manuscript.

Competing interests

The authors declare no competing interests.

Additional information

Supplementary information is available for this paper at <https://doi.org/10.1038/s41929-020-0439-8>.

Correspondence and requests for materials should be addressed to X.H. or X.-Y.L.

Reprints and permissions information is available at www.nature.com/reprints.

Publisher's note Springer Nature remains neutral with regard to jurisdictional claims in published maps and institutional affiliations.

© The Author(s), under exclusive licence to Springer Nature Limited 2020